

**Wildfire-derived pyrogenic carbon modulates riverine
organic matter and biofilm enzyme activities in an in-situ
flume experiment**

Lukas Thuile Bistarelli,¹ Caroline Poyntner,² Cristina Santín,^{3,4} Stefan Helmut Doerr,⁵
Matthew V. Talluto,¹ Gabriel Singer,¹ Gabriel Sigmund^{6*}

¹ Institute of Ecology, University of Innsbruck, Technikerstraße 25, 6020 Innsbruck, Austria

² Institute of Microbiology, University of Innsbruck, Technikerstraße 25, 6020 Innsbruck, Austria

³ Research Unit of Biodiversity, Spanish National Research Council (CSIC), E-33600 Mieres,
Spain

⁴ Swansea University, Department of Biosciences, Singleton Park, Swansea SA2 8PP, UK

⁵ Swansea University, Department of Geography, Singleton Park, Swansea SA2 8PP, UK

⁶ University of Vienna, Department of Environmental Geosciences, Centre for Microbiology and
Environmental Systems Science, Althanstraße 14, 1090 Wien, Austria

Corresponding author: Gabriel Sigmund University of Vienna, Department of Environmental
Geosciences, Centre for Microbiology and Environmental Systems Science, Althanstraße 14,
1090 Wien, Austria e-mail: gabriel.sigmund@univie.ac.at

Abstract

Wildfires produce large amounts of pyrogenic carbon (PyC), including charcoal, known for its chemical recalcitrance and sorption affinity for organic molecules. Wildfire-derived PyC can be transported to fluvial networks. Here it may alter dissolved organic matter (DOM) concentration and composition as well as microbial biofilm functioning. Effects of PyC on carbon cycling in freshwater ecosystems remain poorly investigated. Employing in-stream flumes with a control vs treatment design (PyC pulse addition), we present evidence that field-aged PyC inputs to rivers can increase dissolved organic carbon (DOC) concentration, and alter DOM composition. DOM fluorescence components were not affected by PyC. In-stream DOM composition was altered due to leaching of pyrogenic DOM from PyC and possibly concurrent sorption of riverine DOM to PyC. Decreased DOM aromaticity indicated by lower SUVA₂₄₅ (-0.31 units), and higher pH (0.25 units) were associated with changes in enzymatic activities in benthic biofilms, including a lower recalcitrance index (β -glucosidase/phenol oxidase), suggesting preferential usage of recalcitrant over easily available DOM by biofilms. Particulate PyC deposition onto biofilms may further modulate the impacts of PyC due to direct contact with the biofilm matrix. This study highlights the importance of PyC for in-stream biogeochemical organic matter cycling in fire-affected watersheds.

Keywords

Charcoal, black carbon, dissolved organic carbon, dissolved organic matter, biofilm functioning

1. Introduction

Vegetation fires annually burn ~4 % of Earth's vegetated land surface, forming approximately 256 Tg of pyrogenic carbon (PyC).¹ PyC is a continuum of thermally-altered organic materials, of which a considerable fraction is highly recalcitrant, persisting in the environment for prolonged periods of time.² The chemical composition of PyC is determined by fire conditions (e.g. temperature, charring duration, oxygen availability) and fuel type (e.g. grassy vs woody).³ In fire-affected landscapes fresh as well as aged PyC, in both dissolved and particulate forms, is mobilized to fluvial ecosystems via water erosion.^{4–6} Indeed, significant charcoal presence in river bed deposits in fire affected ecosystems have been the subject of investigation decades ago⁷ and hydrological events (e.g. stormwater runoff) can transport large quantities of PyC into river ecosystems in short periods of time.^{6,8} Coppola and colleagues⁹ found that globally $15.8 \pm 0.9\%$ of riverine particulate organic carbon is of pyrogenic origin. Jones and colleagues¹⁰ estimated that PyC accounts for $12 \pm 5\%$ of the riverine dissolved organic carbon (DOC, i.e., filtered $< 0.45 \mu\text{m}$). PyC is, therefore, a quantitatively substantial fraction of the organic matter component in many river systems.

Rivers do not only transport but also transform organic matter on its way downstream towards the ocean. These transformations can occur via photochemical, microbial, and mechanical processes.^{11–14} Photo-chemical reactions, which are strongly site dependent¹⁵ preferentially degrade highly aromatic dissolved organic matter (DOM) deriving from PyC.¹⁶ In-stream microbiota, especially biofilm communities which are hotspots of microbial functioning, are central to the role of fluvial ecosystems as

bioreactors of terrestrial material,¹⁷ but the microbial degradation of pyrogenic DOM remains poorly understood. Bostick and colleagues¹⁸ recently measured considerable degradation of the labile DOC fraction leached from fresh PyC in laboratory-based experiments, however, the metabolization of fresh as well as aged PyC under natural conditions remains elusive. Finally, mechanical processes can physically disintegrate PyC into smaller particles.¹⁴ This can lead to leaching of particulate as well as dissolved pyrogenic organic matter and metals.^{14,19,20}

The less aromatic, more labile fraction of PyC can be a relevant component of in-stream carbon turnover.^{21,22} Changes in DOC quantity and DOM composition induced by PyC may alter microbial functioning, based on observations in non-fire affected aquatic systems.^{12,23,24} For example, Freixa and colleagues²⁴ showed that shifts in DOM sources (i.e. allochthonous to autochthonous) along the river continuum were accompanied by a change in extracellular enzymatic activities. In addition to pyrogenic DOM, PyC particles can also affect DOM composition and its bioaccessibility by interacting with riverine DOM via selective adsorption. This process has previously been observed for other carbonaceous materials, including carbon-nanomaterials,^{25,26} graphite, and biochar.²⁶

PyC is therefore a common component in limnic systems, with the potential to alter riverine microbial DOM cycling. However, field-based experiments to elucidate specific impacts and processes are still lacking. Here we carry out a field experiment in a natural river to investigate the effects of wildfire-derived PyC inputs on in-stream DOM properties and biofilm functioning. In addition, to our knowledge this study is the first to analyze effects of PyC on in-stream biofilm enzymatic activities. We hypothesized that

PyC would affect (i) in-stream DOM composition and DOC concentration due to sorption of riverine DOM and leaching of pyrogenic DOM leading to a net increase in DOC concentration, and (ii) microbial functions, measured via enzymatic activities by altering substrate composition and pH.

2. Methods

2.1 Site description and field experimental design

This study was carried out at the Austrian river Kleine Ysper (lat 48.218N, long 15.023E), a tributary of the Ysper with a slope of 3.3 cm/m, an average width of 5.47 m \pm 1.44, an upstream catchment area of 68.30 km² at a site situated about 4 km upstream of the confluence with the Danube. This site was selected because the land use in its catchment area is dominated by mixed forest and semi-natural areas which are widespread in the region, and the site has already been characterized in a previous study.²⁷ To our knowledge there are no recorded wildfire occurrences in the upstream catchment area, making this a pristine site for the experiment. Atmospheric PyC inputs are possible, but we found no evidence thereof. The used PyC was selected as a proxy for forest fire-derived PyC. The PyC was charcoal consisting of fully charred woody material from *Pinus sylvestris*, collected from the ground as pieces with a radius of 0.5 – 2.5 cm one year after an extensive wildfire in a pine forest (Karbole, Sweden). This charcoal was produced at an estimated maximum temperature of 800 °C and a charring duration of minimum 200 s.²⁸ Particles were gently crushed, sieved to 0.5 – 1.0 cm, and homogenized. The PyC's molar carbon to nitrogen (C/N) ratio was measured in triplicates on a CHNS analyzer (Vario MACRO, Elementar).

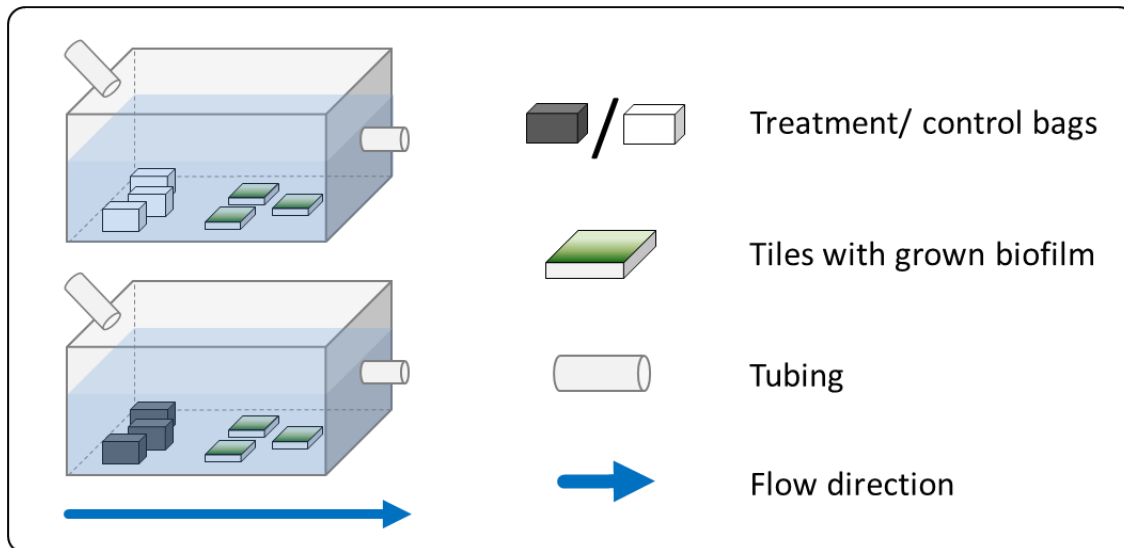


Figure 1: Stream-side flumes setup. Flume design showing bags filled with inert quartz sand (upper) and PyC (lower) for control and treatment, respectively.

For the experiment, 60 ceramic tiles of 25 cm² fixed to a wooden board were exposed on the riverbed from 14th June 2019 to 12th July 2019 for colonization by native biofilm communities. On 12th July 2019, a total of ten experimental in-situ flumes built from commercially available 20-l boxes were placed in the river. Inflow of river water into the flumes was provided using 6 m long tubing (8 mm inner Ø) for each box. The inflow of each tube was placed 5 m upstream of the flumes at a hydraulic head of 20 cm, resulting in an average discharge of $0.47 \pm 0.01 \text{ l min}^{-1}$, which corresponds to a total volume of approximately 225 l passing through each flume over the duration of the experiment (8 h). The water volume in each box was approximately 15 l. A WTW probe was used during each sampling to monitor pH, conductivity, and oxygen concentration in each flume. Biofilm carrying tiles from the river were randomly distributed across the flumes (Fig. 1). Five flumes were used as treatment and control flumes, respectively. 15 paper-filter bags, each containing 15 g of particulate PyC, were added to each treatment flume at the start of the experiment. The amount of PyC added was arbitrarily chosen as a potential post-fire scenario. Actual amounts would depend on site factors

such as fire behavior, amount and type of fuel affected, slope steepness, and size of the hydrological event.^{6,8} The filter bags had a mesh size < 50 µm to allow the release of small PyC particles and DOC. In the control flumes, filter bags without PyC were added to account for potential riverine DOM interactions with the filter bag.

Water samples were collected at each outflow 1, 2, 3, 4, 6, and 8 h after the beginning of the experiment. Additionally, we monitored O₂, pH, and conductivity using a WTW probe (Xylem, Germany). At 1, 4, and 8 h samples were taken for the measurement of total concentrations of Li, Na, Mg, Al, Ca, Sc, Mn, Fe, Co, Zn, Rb, Sr, Y, Mo, Ba, La, Ce, Pr, Nd, Sm, Gd, Dy, Pb, and U (see Figure S1 and Table S1 in the Supporting Information for details).

To assess the deposition of particulate PyC on biofilm surfaces via light microscopical analysis, 20 microscopic glass slides were placed at the bottom of the flumes for the duration of the experiment (see Supporting Information for details).

2.2 PyC leaching experiment

Due to deposition and partial dilution, it was not possible to quantify the leached particulate organic carbon fraction in the flume setup. To overcome this issue, we performed complementary leaching experiments in the laboratory for the duration of the flume-experiment using river water as well as milliQ water. The proportion of PyC and filter bag to water (15 g PyC / l) used in the flume experiments was reproduced in 1 l Schott bottles that were gently agitated with a magnetic stirrer for the same duration than the flume-experiment (8 h, 3 replicates). Filter bags were removed from the bottles and the suspension was shaken to obtain well intermixed water samples for DOC, DOM

properties, and total organic carbon (TOC) measurements. Total Carbon (TC) and inorganic carbon (IC) were measured to calculate TOC ($\text{TOC} = \text{TC} - \text{IC}$) on a TOC-L analyzer (Shimadzu, Japan) using 40 ml vials with a magnetic stirrer to avoid deposition.

2.3 Organic matter properties

To determine DOC concentration and DOM properties, water samples were sterile filtered through pre-washed 0.2 μm Minisart syringe filters (Sartorius, Germany). For DOC measurement we filtered 2 ml of sample into an HPLC vial which was acidified to pH 2 with ultrapure HCl. DOC was analyzed by high temperature combustion on a multi N/C 2100s (Analytik Jena, Germany) with a limit of quantification of 50 $\mu\text{g l}^{-1}$ and a coefficient of variation of 1 – 2%. DOM samples were filtered without any treatment into 10 ml glass vials with PTFE septa. The fluorescent and light absorbing moieties of DOM samples were analyzed spectrofluorometrically on a Horiba Aqualog (Horiba Ltd, Japan), which measures absorbance (250-600 nm, 5 nm increment) and excitation-emission matrices (EEMs, excitation 250-550 nm, emission 250-600 nm, 5 nm increment) concomitantly using a 1 cm quartz cuvette and MilliQ (Millipore, United States) water as optical blank.

We applied absorbance-based measurements to additionally cover DOM components that absorb light but are not fluorescent. The decadal absorption coefficient at 254 nm was used to compute specific UV absorption (SUVA_{254}) which commonly serves as a proxy for aromaticity.²⁹ Rayleigh scatter was deleted from EEMs and Raman scatter was removed by subtracting MQ EEMs from samples EEMs.^{30,31} All EEMs were used for parallel factor analysis (PARAFAC)^{32,33} using the R package staRdom.³⁴ After

exclusion of outliers using the leverage() function in the staRdom routine, 54 EEMs were used to derive 4 fluorescent components, which were compared with literature using the online database OpenFluor.

2.4 Potential extracellular enzymatic activity

Biofilm grown on the submerged tiles was used to perform the potential extracellular enzymatic activity (EEAs) assays reflecting the maximum capacity of an enzyme to cleave a given substrate. We measured the activity of the enzymes β -glucosidase (EC 3.2.1.21), β -xylosidase (EC 3.2.1.37), cellobiohydrolase (EC 3.2.1.91), β -N-acetylglucosaminidase (EC 3.2.1.30), phosphatase (EC 3.1.3.1-2), lipase (EC 3.1.1.3), leucine-aminopeptidase (EC 3.4.11.1), and phenol oxidase (EC 1.10.3). These enzymes are broadly used to understand effects of DOM on bacterial community functioning.^{24,35–42} Enzyme assays were prepared beforehand in deep well plates and brought to the field frozen. At the end of the 8 h field-experiment, we scraped off the biofilm from the submerged tiles using a scalpel and subsequently homogenized it using a frother. An equal amount (300 μ l) of biofilm slurry was used to inoculate each well of the assay which was incubated for 1 h at dark and river temperature. Thereafter, the process was stopped using buffers, and plates were immediately frozen on site. After two days the plates were thawed, gently centrifuged, and analyzed in the laboratory on a Spark plate-reader (Tecan Trading AG, Switzerland). Measured enzymatic activities were used to compute the following enzymatic activity ratios (ERs) as these are biomass independent: Xyl/Glu, which indicates elevated use of large polymeric carbon compounds (e.g. derived from plant material); (Glu+Xyl)/Cbh, indicating the use of easily available polysaccharides over complex polysaccharides; Glu/Pep, indicating a

prevalent use of glucose rather than amino acids as primary carbon source; Glu/Pox, also called recalcitrant index, indicates the use of easily available material over more complex lignin derived material; Pep/Pho indicates whether an ecosystem is rather N limited than P limited; and NAG/Pox indicates the use of easily available C and N over the use of lignin derived C.^{36,37} Further experimental details can be found in the Supporting Information.

2.5 Statistical analysis

To analyze DOC and DOM data, we applied Gaussian process (GP) regressions (code and data can be found at <https://github.com/lukastb/LimnicFires>) as they are able to account for the nonindependence in the response variables that results from the repeated measurements over time. GP regression employs a flexible model structure that can describe the effects of predictors on both the mean and the (auto-) covariance structure of the response variable.⁴³ We employed a simple linear equation for the mean function:

$$E(y) = \alpha + \beta * T \quad \text{eq (1)}$$

where T is an indicator variable indicating whether the treatment was applied; with no covariance and constant variance, this model is nearly identical to a simple linear regression with a categorical predictor.

We modelled covariance within flumes as a decaying function of observation time using a Gaussian kernel function:

$$\text{cov}(y_1, y_2) = \alpha^2 \exp\left(-\frac{(t_1 - t_2)^2}{2\rho^2}\right) + \delta_{ij}\sigma^2 \quad \text{eq (2)}$$

where α and ρ are hyperparameters controlling the variance and bandwidth of the Gaussian process, δ_{ij} is an indicator that is 1 if $i = j$ and 0 otherwise, σ^2 is the residual variance of the response variable y and t is the time of measurement. This kernel generates a variance-covariance matrix where covariance increases as the time between a pair of observations decreases, thus accounting for any autocorrelation due to the repeated measures design of the experiment. We assumed covariance among flumes was zero, and we calibrated a single set of hyperparameters (i.e., α , ρ , and σ) for all flumes, thus assuming that the strength of the time-covariance relationship was identical among flumes. We calibrated the model using the package `rstan`.⁴⁴ We also compared the results of the GPs to generalized linear models (GLMs) with no time dependence and obtained similar parameter estimates. Differences between enzyme ratios in treatment and control flumes were analyzed using t-tests as these data were collected exclusively at the end of the experiment. All uncertainty estimates are provided as standard errors.

3. Results & Discussion

3.1 Pyrogenic carbon increases pH and dissolved organic carbon

pH was elevated by approximately 0.25 units in the treatment flumes compared to the controls after the first 3 h of the experiment and remained nearly constant throughout the remaining 5 h (see Fig. S2a in the Supporting Information). In contrast, O_2 content and conductivity were not strongly affected by PyC addition (see Fig. S2 in the Supporting Information). This is in good agreement with the well-documented alkalinity of biochar – an engineered PyC primarily used in agricultural applications. This alkalinity

234 derives from alkaline surface functional groups on the aromatic PyC structure, as well
 235 as carbonates, and other inorganic moieties in the ash fraction.^{45,46} Metals, which can
 236 occur in the ash fraction, are known to interfere with the functioning of microbial cells by
 237 blocking the active center of enzymes.¹⁹ However, our results indicate that PyC only
 238 slightly affected the concentration of 3 out of 24 metals quantified (see Fig. S1, Table
 239 S1 and S2 in the Supporting Information). This may be because the PyC used was one
 240 year old prior to its deployment in our experiment and, therefore, was depleted from the
 241 easily dissolvable ash fraction during field aging. A slight increase in aqueous
 242 concentration was observed for Mn and Rb, which were likely released from the PyC.
 243 The aqueous concentration of Zn decreased in the presence of PyC, which is consistent
 244 with the increased pH and previous reports on the immobilization of Zn by engineered
 245 PyC such as biochar.⁴⁷

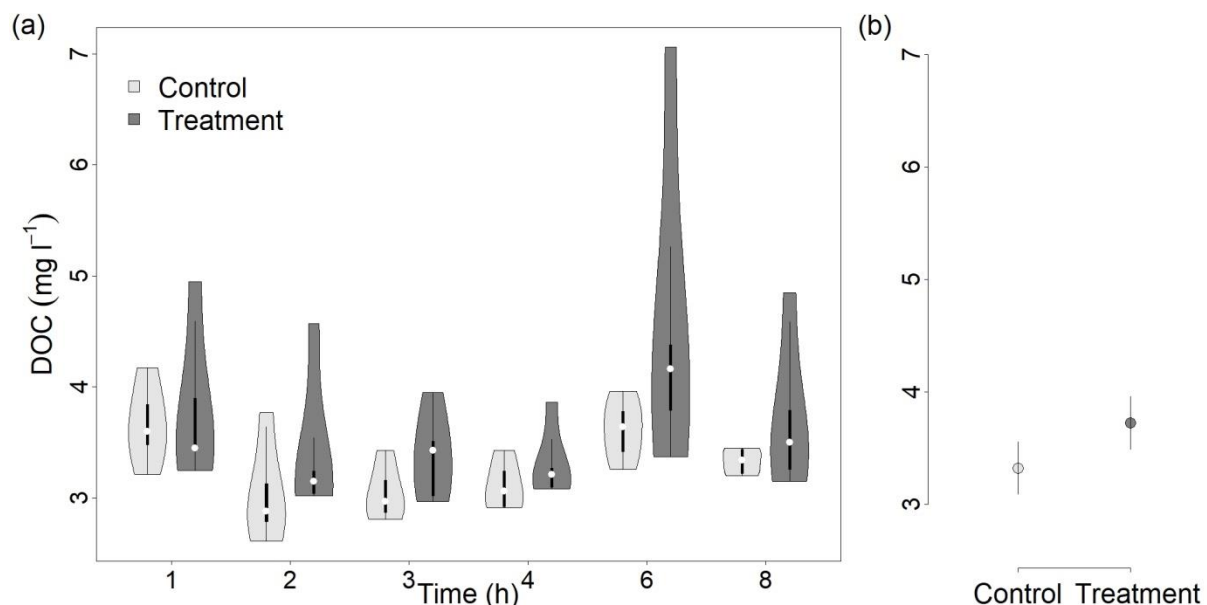


Figure 2: a) DOC concentrations over time in the control and treatment flumes. White dot in box-plots represents median values. b) Mean predicted DOC concentrations based on Gaussian process models for control (light grey) and treatment (dark grey) flumes with 90 % CI. Effect size of 0.4 with 90 % CI (0.07, 0.73).

DOC concentrations across all time points ranged from 2.61 to 4.17, and 2.97 to 7.06 mg l⁻¹ in the control and treatment flumes, respectively. Overall, DOC concentration slightly increased with PyC addition (Fig. 2a, 2b). DOC concentrations were higher in the treatment (mean predicted DOC 3.72 ± 0.14 mg l⁻¹) in comparison to the control (mean predicted DOC 3.32 ± 0.14 mg l⁻¹) flumes, with an overall effect size of 0.40 ± 0.20 mg l⁻¹ based on Gaussian process regression (Fig. 2b). The increases in DOC concentration in treatment flumes can be explained by leaching of pyrogenic organic matter from wildfire charcoals, as also observed in previous laboratory studies.^{18,48,49}

Our results indicate that DOC-leaching from PyC and its physical disintegration exceeds the adsorption of riverine DOC to PyC under conditions such as the ones studied here. Additionally, our measurements are probably a conservative estimate of DOM leaching from PyC in the river water, due to the lower turbulence in flumes compared to the river.

The amount of DOC released from filter bags in the field experiments was estimated as:

$$DOC_{leached} = Q * t * \Delta DOC \quad \text{eq (3)}$$

where Q is the flume-discharge, t the duration of the experiment, and ΔDOC the modelled treatment effect. These calculations indicate that over the 8 h duration of the experiment, at least 89.45 ± 0.30 mg DOC was leached in each flume. As this calculation is assuming no stream DOC was adsorbed, this is a very conservative estimation which corresponds to 0.40 ± 0.01 mg C per g PyC.

Under laboratory conditions each gram of PyC in the filter bag released 0.84 ± 0.01 mg C total organic carbon (TOC) over 8 h (see Table S3 in the Supporting Information), which would correspond to 189.60 ± 1.80 mg TOC in each treatment flume. Considering

this, particulate organic carbon (POC) was computed as $\text{TOC}_{\text{lab}} - \text{DOC}_{\text{flume}}$ and amounted to 0.44 ± 0.01 mg C per g PyC. This represents a conservative estimate of POC as water turbulences and dilution in the flumes are expected to be greater than during the laboratory experiment which could increase POC release. Based on these results, POC also increased upon wildfire char addition. This suggests that the original pieces of charcoal underwent partial disintegration, leading to small particles from the wildfire charcoal being mobilized into river water, which was confirmed by the visual deposition of small PyC particles on the biofilm at the end of the field experiment (see Fig. S3 in the Supporting Information).

Mean POC ($\text{TOC}_{\text{lab}} - \text{DOC}_{\text{flume}}$) and DOC inputs were similar in size amounting to approximately 0.44 ± 0.01 and 0.40 ± 0.01 mg C per g PyC, respectively. Previous studies estimated global PyC fluxes and found that the ratio POC/DOC is approximately $1.5^{2,9,50}$ which is in the range of our findings. Our results show that a considerable amount of carbon can be released from aged PyC particles both in dissolved and particulate forms.

3.2 Pyrogenic carbon addition changes DOM composition

SUVA_{254} , which correlates strongly with aromaticity,²⁹ ranged from 3.09 to 4.71 in the control, and from 1.75 to 4.41 in the treatment flumes. Hence, SUVA_{254} was consistently reduced in presence of PyC, as confirmed by gaussian process regression, which found lower SUVA_{254} in the treatment flumes (mean predicted $\text{SUVA}_{254} = 3.53 \pm 0.11$) in comparison to the control flumes (mean predicted $\text{SUVA}_{254} = 3.84 \pm 0.11$) with an overall effect size of -0.31 ± 0.15 (Fig. 3).

290 PyC consists of both labile and highly aromatic recalcitrant fractions, with the labile
291 fraction being less aromatic and more easily mobilized and degraded by microbes.⁴⁹ In
292 contrast, the highly aromatic fraction is expected to stay longer in the particulate form,
293 constituting a strong sorbent for other aromatic DOM compounds. The notion that labile
294 compounds with low aromaticity are leached from PyC is supported by measured low
295 SUVA₂₅₄ values (2.47 ± 0.17) in MilliQ water leaching experiments (see section 2.3).

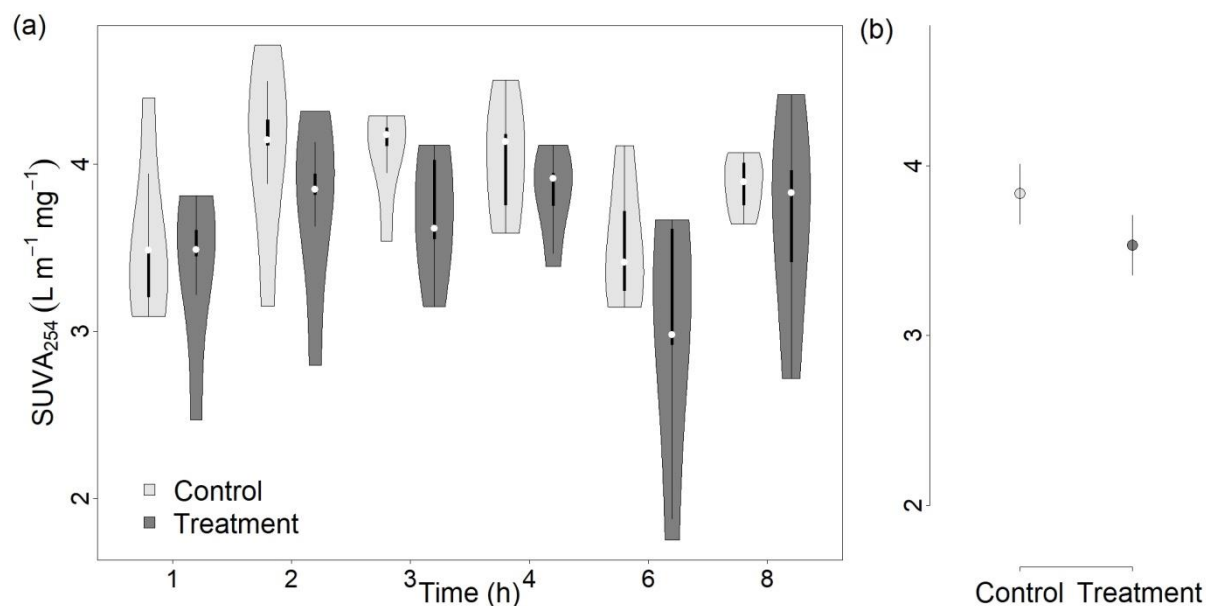


Figure 3: a) SUVA₂₅₄ over time in the control and in the treatment flumes. b) Mean predicted SUVA₂₅₄ based on Gaussian process models for control (light grey) and treatment (dark grey) flumes with 90 % CI. Effect size of -0.31 with 90 % CI (-0.56, -0.05).

296 The reduced SUVA₂₅₄ values in treatment flumes (Fig. 3) could additionally suggest that
297 selective sorption of riverine DOM by PyC simultaneously removed aromatic
298 compounds from the water. This would be in line with recent studies showing that
299 sorption of DOM to PyC particles increases with DOM aromaticity and can be hindered
300 by steric effects excluding very large DOM molecules from reaching certain sorption
301 sites within the charcoal particles.^{26,51}

PARAFAC, a modelling approach used to unravel chemical signatures from EEMs, resulted in the detection of 4 components (see Fig. 4). The PARAFAC report can be found online under the name “LimnicFires” at OpenFluor (<https://openfluor.lablicate.com>) which is a platform for published PARAFAC models.⁵² No significant differences were observed due to PyC additions in any of the 4 components (see Fig. S4 in the Supporting Information).

C1, C2, and C3 are humic-like components whereas C4 is a protein-like component.^{30,53–57} C2 is possibly microbial humic-like based on results from Yamashita and colleagues.⁵⁸ Although not clearly detectable, PARAFAC components suggest that there was a slight increase of mostly humic like chemical compounds following PyC addition (see Fig. S4 in the Supporting Information). This notion is supported by the measured total fluorescence which – albeit not normalized for DOC, slightly increased due to PyC addition (see Fig. S5a in the Supporting Information). When normalized to DOC, patterns invert indicating that a large part of the PyC effect on total fluorescence derives from the increased DOC concentration (see Fig. S5b in the Supporting Information). However, further investigation into PARAFAC components from similar experiments at larger scales and possibly at varying range of PyC concentrations are needed to confirm these interpretations.

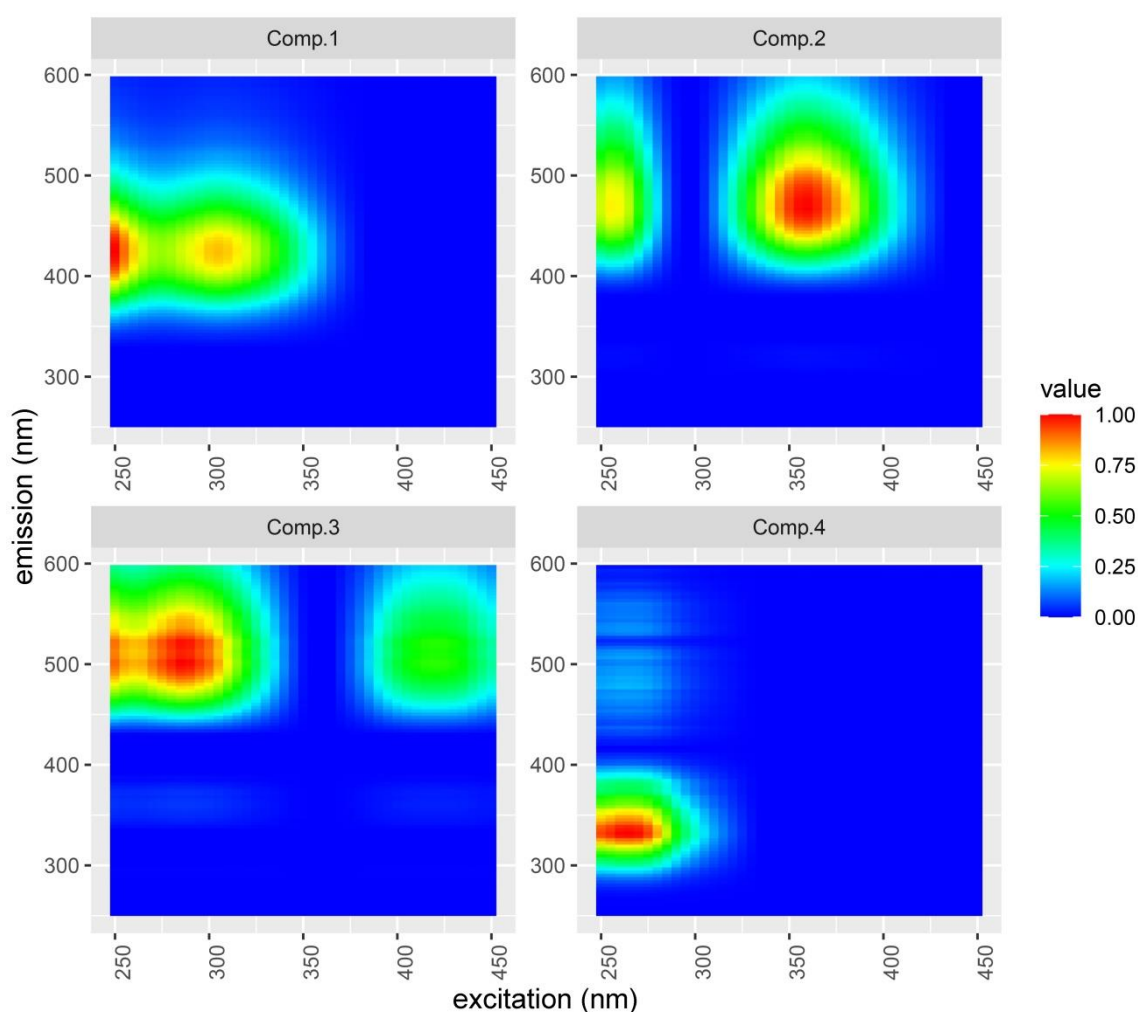


Figure 4: Excitation emission matrices (EEMs) for all four PARAFAC components, modelled from all samples. C1 has its excitation maximum at 250nm and emission maximum at 425nm. C2 has its excitation peak at 360nm and emission peak at 465nm. C3 and C4 have their excitation peak at 285 and 265nm and their emission peaks at 500 and 335nm respectively.

3.3 Pyrogenic carbon addition affects enzymatic activities

Oxidation and hydrolysis are two key processes for DOM degradation. Hydrolytic enzymes degrade non-aromatic DOM structures while oxidative enzymes additionally degrade aromatic DOM structures.⁵⁹ PyC addition significantly decreased the ratio of hydrolytic to oxidative enzymes, indicating a shift towards degradation of aromatic over non-aromatic compounds (see Fig. 5 and Fig. S6 in the Supporting Information).

326 The ERs Xyl/Glu, (Glu+Xyl)/Cbh, Glu/Pox and NAG/Pox, were affected by PyC addition
327 (Fig. 5). Xyl/Glu increased upon PyC addition (t-test, d.f.= 4, p=0.03), indicating a
328 preferential use of large polymeric carbon compounds in comparison to the control
329 flumes. The ratio (Glu+Xyl)/Cbh decreased with PyC addition (t-test, d.f.= 4, p=0.08),
330 indicating a reduced use of easily available polysaccharides in comparison to complex
331 polysaccharides. Glu/Pox, also referred to as the recalcitrance index, decreased with
332 PyC addition (t-test, d.f.= 4, p=0.03), pointing to an increased use of polyphenolic lignin-
333 like compounds in comparison to easily available compounds such as cellobiose or
334 small oligomers.³⁷ In addition, the increased use of rather recalcitrant material is
335 supported by an increased Pox activity and a decreased Glu activity due to PyC
336 addition (see Table S4 in the Supporting Information), although these activities need to
337 be interpreted carefully as they are not normalized for biomass. Lastly, NAG/Pox
338 decreased with PyC addition (t-test, d.f.= 4, p=0.03), indicating an increased use of
339 polyphenolic lignin-like compounds over chitin-derived compounds. Furthermore, the
340 ER variability decreased following PyC addition, especially for the ERs Glu/Pox and
341 NAG/Pox (Fig. 5c, d).

342 Importantly, the large number of particles that settled on the biofilm as observed
343 microscopically (see Fig. S3 in the Supporting Information) may additionally increase
344 PyC effects on enzymatic activity via direct interaction with the biofilm matrix, including
345 the exposure of microbiota to the highly aromatic chemical structure of PyC particles
346 which might have affected the organic matter pool directly available in the biofilm.
347 Particulate bound aromatic organic matter may have induced an increased activity of
348 Pox (Fig. 5 c+d) compared to purely hydrolytic ERs (Fig. 5 a+b), even though such

349 aromatic compounds are generally highly recalcitrant as was recently confirmed in a
 350 laboratory incubation experiment with PyC derived DOM.¹⁸ Furthermore, PyC could
 351 possibly cause oxidative stress to the biofilms via persistent free radicals that have
 352 recently been measured in wildfire derived PyC.²⁸

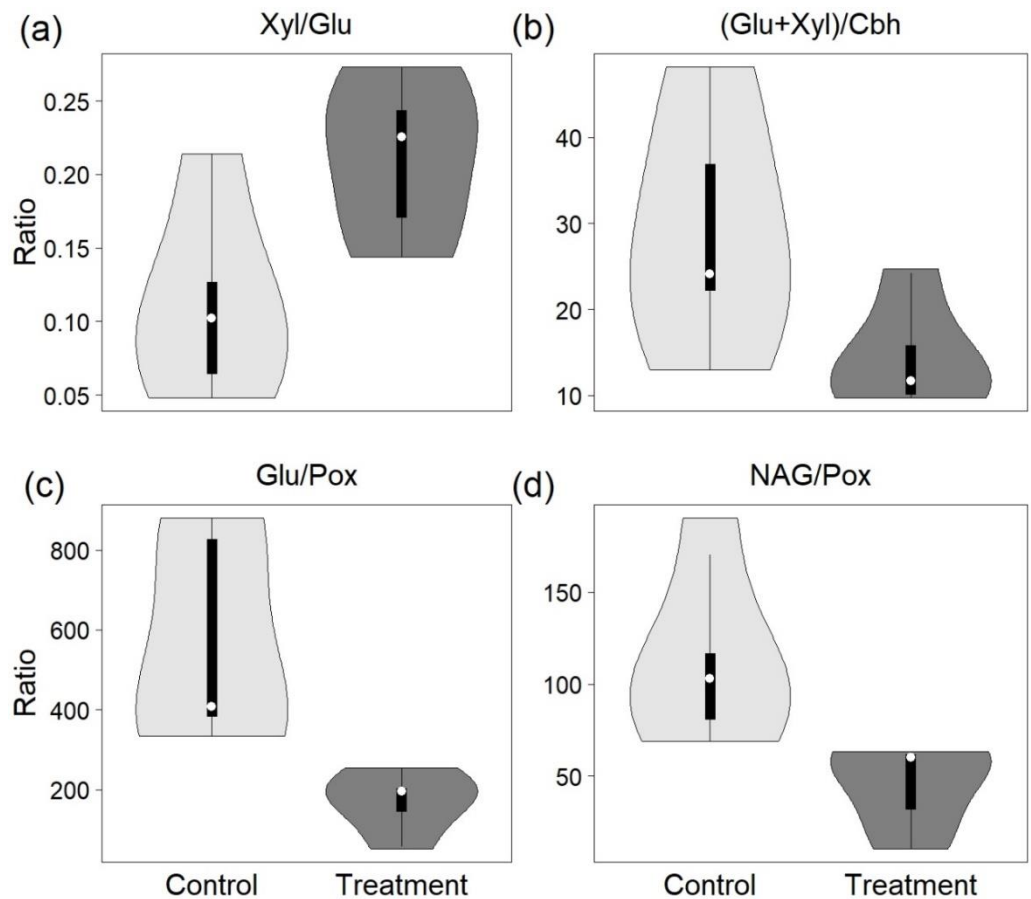


Figure 5: Enzyme ratios without (light grey) and with (dark grey) PyC addition. Xyl = β -xylosidase; Glu = β -glucosidase; Cbh = Cellobiohydrolase; Pox = phenol oxidase; NAG = β -N-acetyl-glucosaminidase (a) Xyl/Glu ratio; (b) (Glu+Xyl)/Cbh ratio; (c) Glu/Pox ratio i.e. recalcitrant index; (d) NAG/Pox ratio.

353 Observed alterations of ERs in benthic biofilms with PyC addition can be explained by
 354 the combined effect of changes in DOC quantity, DOM quality, and pH. These findings
 355 are in line with studies on potential drivers of ER variability.^{24,35,38,60} For instance, in a
 356 meta-analysis comparing terrestrial, marine, and freshwater ecosystems, Arnosti and
 357 colleagues⁶⁰ found that pH is more important in controlling enzymatic activities in

freshwater ecosystems in comparison to marine environments. Freixa and colleagues²⁴ related enzymatic activities in a longitudinal river continuum to the change in DOM composition from up – to downstream and found that enzymatic activities reflect a transition from allochthonous to autochthonous DOM along the river continuum.

In this study, which used field aged wildfire charcoal that was likely depleted from mobile metals due to leaching in the field, the small changes in metal concentration observed very likely did not have an effect on enzyme activities. For example, Zn has been shown to inhibit β -glucosidase activity of in-stream biofilms.⁶¹ Thus, based on the slightly lower Zn concentration measured in the treatment flumes, PyC could be expected to lead to an increase in the recalcitrant index (i.e. Glu/Pox ratio). However, we observed the opposite pattern (Fig. 5c), likely because other factors, including DOM composition were more important for biofilm functioning. Future experiments using ash-rich and fresh PyC will be necessary to elucidate effects on biofilm functioning of metals that can be mobilized during wildfires.

The ERs in this study indicate that PyC addition led to an overall compositional change of DOM towards lower biodegradability, although DOC increased (Fig. 2) and DOM aromaticity decreased (Fig. 3). This is in line with studies on non-wildfire affected streams reporting changes in enzymatic activity in dependence of OM substrate composition.²⁴ At first it may appear contradictory that upon PyC addition, ERs indicate a decrease in easily assimilable DOM while SUVA₂₅₄ indicates a decreased DOM aromaticity. Aromaticity, however, is not the only DOM property linked to recalcitrance and decreased degradability. For instance, molecular size, aqueous solubility, oxidation

state, molecular complexity, as well as the lack of N-containing substituents are also linked to the recalcitrance of organic matter.⁶²

Here we show that in this field-based experiment, the input of PyC increases riverine DOC concentrations, changes DOM composition, and modifies biofilm enzyme activities. Our results therefore indicate that PyC can alter fluvial carbon cycling, albeit magnitude and transferability of our results needs further investigation, especially in other rivers and at larger spatial and temporal scales.

4. Implications

Water erosion and colloidal transport of PyC into limnic systems can introduce substantial changes in DOC concentration and DOM composition. We here report on the release of organic matter from PyC with the potential simultaneous selective adsorption of native aromatic substances from riverine DOM in a natural river system. Our results indicate that PyC, both in particulate and dissolved form, affect enzymatic activities in benthic biofilms – especially for oxidative enzymes. PyC addition increased pH, which can also play a role in altering enzymatic activities. Lastly, deposition of particulate PyC directly on the biofilm surface brings the PyC in close contact with the biofilm matrix, potentially modulating the aforementioned effects. Overall, our results suggest that PyC inputs into freshwater can directly affect enzymatic activities, thus altering in-stream benthic biofilm functioning and carbon cycling. Our in-stream flume approach, applied here for the first time, can be adapted to study a diverse range of rivers, enabling a more comprehensive understanding of wildfire effects on riverine carbon cycling. Further experiments varying the amount of PyC could be used to

construct dose-response curves, and changing the exposure time could help gain insights into changes in enzymatic activity over time. In addition, in future experiments ^{13}C labelled PyC could be used to differentiate DOM from PyC from riverine DOM, potentially providing valuable additional insights into mechanism at play.

Acknowledgement

This study was partially funded within the ERC Starting Grant FLUFLUX (grant number ERC-STG 716196 to GSinger). PyC sample collection was supported by FORMAS grant FR-2019/0007 (CSantin & SHDoerr). We would like to thank Tobias Goldhammer and Sarah Krockner of the chemical laboratory (CAB) at the Leibniz-Institute of Freshwater Ecology and Inland Fisheries (IGB) for measuring DOC concentrations. We would like to thank the University of Natural Resources and Life Sciences, Department of Biotechnology, for using their microscope equipment.

References

- (1) van der Werf, G. R.; Randerson, J. T.; Giglio, L.; van Leeuwen, T. T.; Chen, Y.; Rogers, B. M.; Mu, M.; van Marle, M. J. E.; Morton, D. C.; Collatz, G. J.; Yokelson, R. J.; Kasibhatla, P. S. Global Fire Emissions Estimates during 1997–2016. *Earth Syst. Sci. Data* **2017**, 9 (2), 697–720. <https://doi.org/10.5194/essd-9-697-2017>.
- (2) Jones, M. W.; Santín, C.; van der Werf, G. R.; Doerr, S. H. Global Fire Emissions Buffered by the Production of Pyrogenic Carbon. *Nat. Geosci.* **2019**, 12 (9), 742–747. <https://doi.org/10.1038/s41561-019-0403-x>.

- 423 (3) Santín, C.; Doerr, S. H.; Merino, A.; Bucheli, T. D.; Bryant, R.; Ascough, P.; Gao,
424 X.; Masiello, C. A. Carbon Sequestration Potential and Physicochemical
425 Properties Differ between Wildfire Charcoals and Slow-Pyrolysis Biochars. *Sci.*
426 *Rep.* **2017**, 7 (1), 11233. <https://doi.org/10.1038/s41598-017-10455-2>.
- 427 (4) Santín, C.; Doerr, S. H.; Kane, E. S.; Masiello, C. A.; Ohlson, M.; de la Rosa, J.
428 M.; Preston, C. M.; Dittmar, T. Towards a Global Assessment of Pyrogenic
429 Carbon from Vegetation Fires. *Glob. Chang. Biol.* **2016**, 22 (1), 76–91.
430 <https://doi.org/10.1111/gcb.12985>.
- 431 (5) Dittmar, T.; de Rezende, C. E.; Manecki, M.; Niggemann, J.; Coelho Ovalle, A. R.;
432 Stubbins, A.; Bernardes, M. C. Continuous Flux of Dissolved Black Carbon from a
433 Vanished Tropical Forest Biome. *Nat. Geosci.* **2012**, 5 (9), 618–622.
434 <https://doi.org/10.1038/ngeo1541>.
- 435 (6) Bellè, S.-L.; Berhe, A. A.; Hagedorn, F.; Santin, C.; Schiedung, M.; van Meerveld,
436 I.; Abiven, S. Key Drivers of Pyrogenic Carbon Redistribution during a Simulated
437 Rainfall Event. *Biogeosciences* **2021**, 18 (3), 1105–1126.
438 <https://doi.org/10.5194/bg-18-1105-2021>.
- 439 (7) Blong, R. J.; Gillespie, R. Fluvially Transported Charcoal Gives Erroneous ¹⁴C
440 Ages for Recent Deposits. *Nature* **1978**, 271 (February), 739–741.
- 441 (8) Masiello, C. A.; Berhe, A. A. First Interactions with the Hydrologic Cycle
442 Determine Pyrogenic Carbon's Fate in the Earth System. *Earth Surf. Process.*
443 *Landforms* **2020**, 45 (10), 2394–2398. <https://doi.org/10.1002/esp.4925>.

- 444 (9) Coppola, A. I.; Wiedemeier, D. B.; Galy, V.; Haghipour, N.; Hanke, U. M.;
445 Nascimento, G. S.; Usman, M.; Blattmann, T. M.; Reisser, M.; Freymond, C. V.;
446 Zhao, M.; Voss, B.; Wacker, L.; Schefuß, E.; Peucker-Ehrenbrink, B.; Abiven, S.;
447 Schmidt, M. W. I.; Eglinton, T. I. Global-Scale Evidence for the Refractory Nature
448 of Riverine Black Carbon. *Nat. Geosci.* **2018**, *11* (8), 584–588.
449 <https://doi.org/10.1038/s41561-018-0159-8>.
- 450 (10) Jones, M. W.; Coppola, A. I.; Santín, C.; Dittmar, T.; Jaffé, R.; Doerr, S. H.; Quine,
451 T. A. Fires Prime Terrestrial Organic Carbon for Riverine Export to the Global
452 Oceans. *Nat. Commun.* **2020**, *11* (1), 2791. [https://doi.org/10.1038/s41467-020-](https://doi.org/10.1038/s41467-020-16576-z)
453 [16576-z](https://doi.org/10.1038/s41467-020-16576-z).
- 454 (11) Cole, J. J.; Prairie, Y. T.; Caraco, N. F.; McDowell, W. H.; Tranvik, L. J.; Striegl, R.
455 G.; Duarte, C. M.; Kortelainen, P.; Downing, J. a.; Middelburg, J. J.; Melack, J.
456 Plumbing the Global Carbon Cycle: Integrating Inland Waters into the Terrestrial
457 Carbon Budget. *Ecosystems* **2007**, *10* (1), 172–185.
458 <https://doi.org/10.1007/s10021-006-9013-8>.
- 459 (12) Battin, T. J.; Kaplan, L. A.; Findlay, S.; Hopkinson, C. S.; Marti, E.; Packman, A. I.;
460 Newbold, J. D.; Sabater, F. Biophysical Controls on Organic Carbon Fluxes in
461 Fluvial Networks. *Nat. Geosci.* **2008**, *1* (2), 95–100.
462 <https://doi.org/10.1038/ngeo101>.
- 463 (13) Fasching, C.; Behounek, B.; Singer, G.; Battin, T. J. Microbial Degradation of
464 Terrigenous Dissolved Organic Matter and Potential Consequences for Carbon
465 Cycling in Brown-Water Streams. *Sci. Rep.* **2014**, *4*, 4981.

466 <https://doi.org/10.1038/srep04981>.

467 (14) Sigmund, G.; Jiang, C.; Hofmann, T.; Chen, W. Environmental Transformation of
468 Natural and Engineered Carbon Nanoparticles and Implications for the Fate of
469 Organic Contaminants. *Environ. Sci. Nano* **2018**, *5* (11), 2500–2518.
470 <https://doi.org/10.1039/C8EN00676H>.

471 (15) Panneer Selvam, B.; Lapierre, J.-F.; Soares, A. R. A.; Bastviken, D.; Karlsson, J.;
472 Berggren, M. Photo-Reactivity of Dissolved Organic Carbon in the Freshwater
473 Continuum. *Aquat. Sci.* **2019**, *81* (4), 57. [https://doi.org/10.1007/s00027-019-](https://doi.org/10.1007/s00027-019-0653-0)
474 [0653-0](https://doi.org/10.1007/s00027-019-0653-0).

475 (16) Bostick, K. W.; Zimmerman, A. R.; Goranov, A. I.; Mitra, S.; Hatcher, P. G.;
476 Wozniak, A. S. Photolability of Pyrogenic Dissolved Organic Matter from a
477 Thermal Series of Laboratory-Prepared Chars. *Sci. Total Environ.* **2020**, *724*,
478 138198. <https://doi.org/10.1016/j.scitotenv.2020.138198>.

479 (17) Battin, T. J.; Besemer, K.; Bengtsson, M. M.; Romani, A. M.; Packmann, A. I. The
480 Ecology and Biogeochemistry of Stream Biofilms. *Nat. Rev. Microbiol.* **2016**, *14*
481 (4), 251–263. <https://doi.org/10.1038/nrmicro.2016.15>.

482 (18) Bostick, K. W.; Zimmerman, A. R.; Goranov, A. I.; Mitra, S.; Hatcher, P. G.;
483 Wozniak, A. S. Biolability of Fresh and Photodegraded Pyrogenic Dissolved
484 Organic Matter From Laboratory-Prepared Chars. *J. Geophys. Res.*
485 *Biogeosciences* **2021**, *126* (5), 1–17. <https://doi.org/10.1029/2020JG005981>.

486 (19) Lemire, J. A.; Harrison, J. J.; Turner, R. J. Antimicrobial Activity of Metals:

487 Mechanisms, Molecular Targets and Applications. *Nat. Rev. Microbiol.* **2013**, 11
 488 (6), 371–384. <https://doi.org/10.1038/nrmicro3028>.

489 (20) Smith, H. G.; Sheridan, G. J.; Lane, P. N. J.; Nyman, P.; Haydon, S. Wildfire
 490 Effects on Water Quality in Forest Catchments: A Review with Implications for
 491 Water Supply. *J. Hydrol.* **2011**, 396 (1–2), 170–192.
 492 <https://doi.org/10.1016/j.jhydrol.2010.10.043>.

493 (21) Norwood, M. J.; Louchouart, P.; Kuo, L. J.; Harvey, O. R. Characterization and
 494 Biodegradation of Water-Soluble Biomarkers and Organic Carbon Extracted from
 495 Low Temperature Chars. *Org. Geochem.* **2013**, 56, 111–119.
 496 <https://doi.org/10.1016/j.orggeochem.2012.12.008>.

497 (22) Myers-Pigg, A. N.; Louchouart, P.; Amon, R. M. W.; Prokushkin, A.; Pierce, K.;
 498 Rubtsov, A. Labile Pyrogenic Dissolved Organic Carbon in Major Siberian Arctic
 499 Rivers: Implications for Wildfire-Stream Metabolic Linkages. *Geophys. Res. Lett.*
 500 **2015**, 42 (2), 377–385. <https://doi.org/10.1002/2014GL062762>.

501 (23) Judd, K. E.; Crump, B. C.; Kling, G. W. Variation in Dissolved Organic Matter
 502 Controls Bacterial Production and Community Composition. *Ecology* **2006**, 87 (8),
 503 2068–2079. [https://doi.org/10.1890/0012-9658\(2006\)87\[2068:vidomc\]2.0.co;2](https://doi.org/10.1890/0012-9658(2006)87[2068:vidomc]2.0.co;2).

504 (24) Freixa, A.; Ejarque, E.; Crognale, S.; Amalfitano, S.; Fazi, S.; Butturini, A.;
 505 Romaní, A. M. Sediment Microbial Communities Rely on Different Dissolved
 506 Organic Matter Sources along a Mediterranean River Continuum. *Limnol.*
 507 *Oceanogr.* **2016**, 61 (4), 1389–1405. <https://doi.org/10.1002/lno.10308>.

- 508 (25) Ateia, M.; Apul, O. G.; Shimizu, Y.; Muflihah, A.; Yoshimura, C.; Karanfil, T.
509 Elucidating Adsorptive Fractions of Natural Organic Matter on Carbon Nanotubes.
510 *Environ. Sci. Technol.* **2017**, *51* (12), 7101–7110.
511 <https://doi.org/10.1021/acs.est.7b01279>.
- 512 (26) Castan, S.; Sigmund, G.; Hüffer, T.; Tepe, N.; von der Kammer, F.; Chefetz, B.;
513 Hofmann, T. The Importance of Aromaticity to Describe the Interactions of
514 Organic Matter with Carbonaceous Materials Depends on Molecular Weight and
515 Sorbent Geometry. *Environ. Sci. Process. Impacts* **2020**, *22* (9), 1888–1897.
516 <https://doi.org/10.1039/D0EM00267D>.
- 517 (27) Fuß, T.; Behounek, B.; Ulseth, A. J.; Singer, G. A. Land Use Controls Stream
518 Ecosystem Metabolism by Shifting Dissolved Organic Matter and Nutrient
519 Regimes. *Freshw. Biol.* **2017**, *62* (3), 582–599. <https://doi.org/10.1111/fwb.12887>.
- 520 (28) Sigmund, G.; Santín, C.; Pignitter, M.; Tepe, N.; Doerr, S. H.; Hofmann, T.
521 Environmentally Persistent Free Radicals Are Ubiquitous in Wildfire Charcoals
522 and Remain Stable for Years. *Commun. Earth Environ.* **2021**, *2* (1), 68.
523 <https://doi.org/10.1038/s43247-021-00138-2>.
- 524 (29) Weishaar, J. L.; Aiken, G. R.; Bergamaschi, B. A.; Fram, M. S.; Fujii, R.; Mopper,
525 K. Evaluation of Specific Ultraviolet Absorbance as an Indicator of the Chemical
526 Composition and Reactivity of Dissolved Organic Carbon. *Environ. Sci. Technol.*
527 **2003**, *37* (20), 4702–4708. <https://doi.org/10.1021/es030360x>.
- 528 (30) Parlanti, E.; Wörz, K.; Geoffroy, L.; Lamotte, M. Dissolved Organic Matter
529 Fluorescence Spectroscopy as a Tool to Estimate Biological Activity in a Coastal

530 Zone Submitted to Anthropogenic Inputs. *Org. Geochem.* **2000**, 31 (12), 1765–
531 1781. [https://doi.org/10.1016/S0146-6380\(00\)00124-8](https://doi.org/10.1016/S0146-6380(00)00124-8).

532 (31) McKnight, D. M.; Boyer, E. W.; Westerhoff, P. K.; Doran, P. T.; Kulbe, T.;
533 Andersen, D. T. Spectrofluorometric Characterization of Dissolved Organic Matter
534 for Indication of Precursor Organic Material and Aromaticity. *Limnol. Oceanogr.*
535 **2001**, 46 (1), 38–48. <https://doi.org/10.4319/lo.2001.46.1.0038>.

536 (32) Murphy, K. R.; Stedmon, C. A.; Graeber, D.; Bro, R. Fluorescence Spectroscopy
537 and Multi-Way Techniques. PARAFAC. *Anal. Methods* **2013**, 5 (23), 6557.
538 <https://doi.org/10.1039/c3ay41160e>.

539 (33) Pucher, M.; Wünsch, U.; Weigelhofer, G.; Murphy, K.; Hein, T.; Graeber, D.
540 StaRdom: Versatile Software for Analyzing Spectroscopic Data of Dissolved
541 Organic Matter in R. *Water* **2019**, 11 (11), 2366.
542 <https://doi.org/10.3390/w11112366>.

543 (34) Pucher, M.; Graeber, D. StaRdom: PARAFAC Analysis on DOM EEMs,
544 Calculating Absorbance Slopes. <https://Github.Com/MatthiasPucher/StaRdom>.
545 2019 (accessed February 14th, 2021).

546 (35) Stark, S.; Männistö, M. K.; Eskelinen, A. Nutrient Availability and PH Jointly
547 Constrain Microbial Extracellular Enzyme Activities in Nutrient-Poor Tundra Soils.
548 *Plant Soil* **2014**, 383 (1–2), 373–385. <https://doi.org/10.1007/s11104-014-2181-y>.

549 (36) Ylla, I.; Peter, H.; Romani, A. M.; Tranvik, L. J. Different Diversity-Functioning
550 Relationship in Lake and Stream Bacterial Communities. *FEMS Microbiol. Ecol.*

551 **2013**, 85 (1), 95–103. <https://doi.org/10.1111/1574-6941.12101>.

552 (37) Sinsabaugh, R. L.; Follstad Shah, J. J. Eoenzymatic Stoichiometry of
553 Recalcitrant Organic Matter Decomposition: The Growth Rate Hypothesis in
554 Reverse. *Biogeochemistry* **2011**, 102 (1–3), 31–43.
555 <https://doi.org/10.1007/s10533-010-9482-x>.

556 (38) Romaní, A. M.; Guasch, H.; Munoz, I.; Ruana, J.; Vilalta, E.; Schwartz, T.;
557 Emtiazi, F.; Sabater, S. Biofilm Structure and Function and Possible Implications
558 for Riverine DOC Dynamics. *Microb. Ecol.* **2004**, 47 (4), 316–328.
559 <https://doi.org/10.1007/s00248-003-2019-2>.

560 (39) Romaní, A. M.; Vázquez, E.; Butturini, A. Microbial Availability and Size
561 Fractionation of Dissolved Organic Carbon After Drought in an Intermittent
562 Stream: Biogeochemical Link Across the Stream–Riparian Interface. *Microb. Ecol.*
563 **2006**, 52 (3), 501–512. <https://doi.org/10.1007/s00248-006-9112-2>.

564 (40) Sinsabaugh, R. L.; Follstad Shah, J. J.; Hill, B. H.; Elonen, C. M. Eoenzymatic
565 Stoichiometry of Stream Sediments with Comparison to Terrestrial Soils.
566 *Biogeochemistry* **2012**, 111 (1–3), 455–467. [https://doi.org/10.1007/s10533-011-](https://doi.org/10.1007/s10533-011-9676-x)
567 9676-x.

568 (41) Romaní, A. M.; Fischer, H.; Mille-lindblom, C.; Tranvik, L. J.; Roman, A. M.;
569 Fischer, H.; Mille-lindblom, C.; Tranvik, L. J. Interactions of Bacteria and Fungi on
570 Decomposing Litter : Differential Extracellular Enzyme Activities. *Ecology* **2006**, 87
571 (10), 2559–2569. [https://doi.org/10.1890/0012-](https://doi.org/10.1890/0012-9658(2006)87[2559:IOBAFO]2.0.CO;2)
572 9658(2006)87[2559:IOBAFO]2.0.CO;2.

- 573 (42) Romani, A. M.; Sabater, S. Structure and Activity of Rock and Sand Biofilms in a
574 Mediterranean Stream. *Ecology* **2001**, 82 (11), 3232–3245.
575 [https://doi.org/https://doi.org/10.1890/0012-](https://doi.org/https://doi.org/10.1890/0012-9658(2001)082[3232:SAAORA]2.0.CO;2)
576 [9658\(2001\)082\[3232:SAAORA\]2.0.CO;2](https://doi.org/https://doi.org/10.1890/0012-9658(2001)082[3232:SAAORA]2.0.CO;2).
- 577 (43) Rasmussen, C. E.; Williams, C. K. I. Gaussian Processes for Machine Learning
578 (Adaptive Computation and Machine Learning). *MIT Press* **2005**.
- 579 (44) Stan Development Team. Stan Development Team (2019). RStan: The R
580 Interface to Stan. R Package Version 2.19.2. [Http://Mc-Stan.Org/](http://Mc-Stan.Org/). 2019 (accessed
581 February 14th, 2021).
- 582 (45) Fidel, R. B.; Laird, D. A.; Thompson, M. L.; Lawrinenko, M. Characterization and
583 Quantification of Biochar Alkalinity. *Chemosphere* **2017**, 167, 367–373.
584 <https://doi.org/10.1016/j.chemosphere.2016.09.151>.
- 585 (46) Bodí, M. B.; Martin, D. A.; Balfour, V. N.; Santín, C.; Doerr, S. H.; Pereira, P.;
586 Cerdà, A.; Mataix-Solera, J. Wildland Fire Ash: Production, Composition and Eco-
587 Hydro-Geomorphic Effects. *Earth-Science Rev.* **2014**, 130, 103–127.
588 <https://doi.org/10.1016/j.earscirev.2013.12.007>.
- 589 (47) Cairns, S.; Robertson, I.; Sigmund, G.; Street-Perrott, A. The Removal of Lead,
590 Copper, Zinc and Cadmium from Aqueous Solution by Biochar and Amended
591 Biochars. *Environ. Sci. Pollut. Res.* **2020**, 27 (17), 21702–21715.
592 <https://doi.org/10.1007/s11356-020-08706-3>.
- 593 (48) Bostick, K. W.; Zimmerman, A. R.; Wozniak, A. S.; Mitra, S.; Hatcher, P. G.

- 594 Production and Composition of Pyrogenic Dissolved Organic Matter From a
595 Logical Series of Laboratory-Generated Chars. *Front. Earth Sci.* **2018**, 6 (April),
596 1–14. <https://doi.org/10.3389/feart.2018.00043>.
- 597 (49) Abiven, S.; Hengartner, P.; Schneider, M. P. W.; Singh, N.; Schmidt, M. W. I.
598 Pyrogenic Carbon Soluble Fraction Is Larger and More Aromatic in Aged
599 Charcoal than in Fresh Charcoal. *Soil Biol. Biochem.* **2011**, 43 (7), 1615–1617.
600 <https://doi.org/10.1016/j.soilbio.2011.03.027>.
- 601 (50) Jaffé, R.; Ding, Y.; Niggemann, J.; Vähätalo, A. V.; Stubbins, A.; Spencer, R. G.
602 M.; Campbell, J.; Dittmar, T. Global Charcoal Mobilization from Soils via
603 Dissolution and Riverine Transport to the Oceans. *Science* (80-.). **2013**, 340
604 (6130), 345–347. <https://doi.org/10.1126/science.1231476>.
- 605 (51) Engel, M.; Chefetz, B. Adsorptive Fractionation of Dissolved Organic Matter
606 (DOM) by Carbon Nanotubes. *Environ. Pollut.* **2015**, 197, 287–294.
607 <https://doi.org/10.1016/j.envpol.2014.11.020>.
- 608 (52) Murphy, K. R.; Stedmon, C. A.; Wenig, P.; Bro, R. OpenFluor– an Online Spectral
609 Library of Auto-Fluorescence by Organic Compounds in the Environment. *Anal.*
610 *Methods* **2014**, 6 (3), 658–661. <https://doi.org/10.1039/C3AY41935E>.
- 611 (53) Coble, P. G. Characterization of Marine and Terrestrial DOM in Seawater Using
612 Excitation-Emission Matrix Spectroscopy. *Mar. Chem.* **1996**, 51 (4), 325–346.
613 [https://doi.org/10.1016/0304-4203\(95\)00062-3](https://doi.org/10.1016/0304-4203(95)00062-3).
- 614 (54) Coble, P. G.; Green, S. A.; Blough, N. V.; Gagosian, R. B. Characterization of

615 Dissolved Organic Matter in the Black Sea by Fluorescence Spectroscopy. *Nature*
616 **1990**, 348 (6300), 432–435. <https://doi.org/10.1038/348432a0>.

617 (55) Murphy, K. R.; Ruiz, G. M.; Dunsmuir, W. T. M.; Waite, T. D. Optimized
618 Parameters for Fluorescence-Based Verification of Ballast Water Exchange by
619 Ships. *Environ. Sci. Technol.* **2006**, 40 (7), 2357–2362.
620 <https://doi.org/10.1021/es0519381>.

621 (56) Fellman, J. B.; Hood, E.; Spencer, R. G. M. Fluorescence Spectroscopy Opens
622 New Windows into Dissolved Organic Matter Dynamics in Freshwater
623 Ecosystems: A Review. *Limnol. Oceanogr.* **2010**, 55 (6), 2452–2462.
624 <https://doi.org/10.4319/lo.2010.55.6.2452>.

625 (57) Singh, S.; Inamdar, S.; Scott, D. Comparison of Two PARAFAC Models of
626 Dissolved Organic Matter Fluorescence for a Mid-Atlantic Forested Watershed in
627 the USA. *J. Ecosyst.* **2013**, 2013, 1–16. <https://doi.org/10.1155/2013/532424>.

628 (58) Yamashita, Y.; Fichot, C. G.; Shen, Y.; Jaffé, R.; Benner, R. Linkages among
629 Fluorescent Dissolved Organic Matter, Dissolved Amino Acids and Lignin-Derived
630 Phenols in a River-Influenced Ocean Margin. *Front. Mar. Sci.* **2015**, 2 (NOV), 1–
631 14. <https://doi.org/10.3389/fmars.2015.00092>.

632 (59) Romani, A. M.; Artigas, J.; Ylla, I. Extracellular Enzymes in Aquatic Biofilms:
633 Microbial Interactions versus Water Quality Effects in the Use of Organic Matter.
634 *Microb. biofilms* **2012**, 153–174.

635 (60) Arnosti, C.; Bell, C.; Moorhead, D. L.; Sinsabaugh, R. L.; Steen, A. D.;

636 Stromberger, M.; Wallenstein, M.; Weintraub, M. N. Extracellular Enzymes in
637 Terrestrial, Freshwater, and Marine Environments: Perspectives on System
638 Variability and Common Research Needs. *Biogeochemistry* **2014**, 117 (1), 5–21.
639 <https://doi.org/10.1007/s10533-013-9906-5>.

640 (61) Fechner, L. C.; Gourlay-Francé, C.; Uher, E.; Tusseau-Vuillemin, M.-H. Adapting
641 an Enzymatic Toxicity Test to Allow Comparative Evaluation of Natural
642 Freshwater Biofilms' Tolerance to Metals. *Ecotoxicology* **2010**, 19 (7), 1302–1311.
643 <https://doi.org/10.1007/s10646-010-0517-9>.

644 (62) Kleber, M. What Is Recalcitrant Soil Organic Matter? *Environ. Chem.* **2010**, 7 (4),
645 320. <https://doi.org/10.1071/EN10006>.

646